Electronic Supplementary Information

Confinement boosts CO oxidation on Ni atom embedded inside boron nitride nanotubes

Yadong Zhang,[†,‖] *Yuzhen Liu,*[†,‖] *Zhaoshun Meng,*[†] *Cai Ning,*[†] *Chuanyun Xiao,*[†] *Kaiming Deng,*[†]

Purusottam Jena,[*,‡] *and Ruifeng Lu*[*,†,§]

[†]Department of Applied Physics, Nanjing University of Science and Technology, Nanjing 210094, People's Republic of China

[‡]Department of Physics, Virginia Commonwealth University, Richmond, Virginia 23284, United States

[§]State Key Lab of Molecular Reaction Dynamics, Dalian Institute of Chemical Physics, Chinese Academy of Sciences, Dalian 116023, People's Republic of China

Corresponding Author

*E-mail: rflu@njust.edu.cn (R.F.L.).

*E-mail: pjena@vcu.edu (P.J.).

[‖]These authors contributed equally to this work

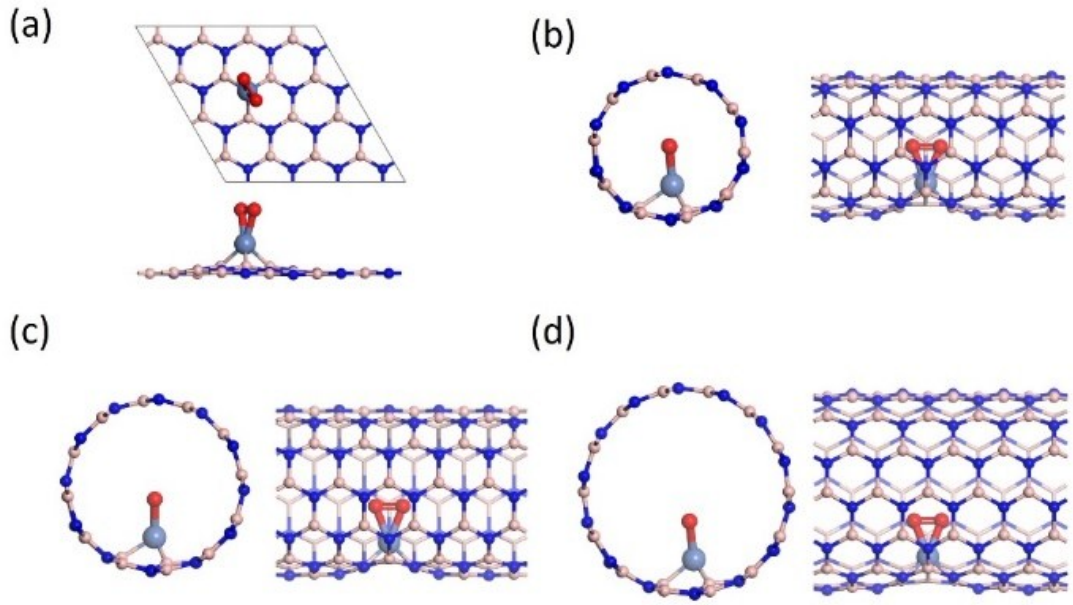

Figure S1. The optimized molecular configurations of O_2 adsorption on the Ni atom embedded on the (a) surface of h-BN, (b) interior walls of BNNT(5, 5), (c) BNNT(6, 6), and (d) BNNT (7, 7) with N vacancy.

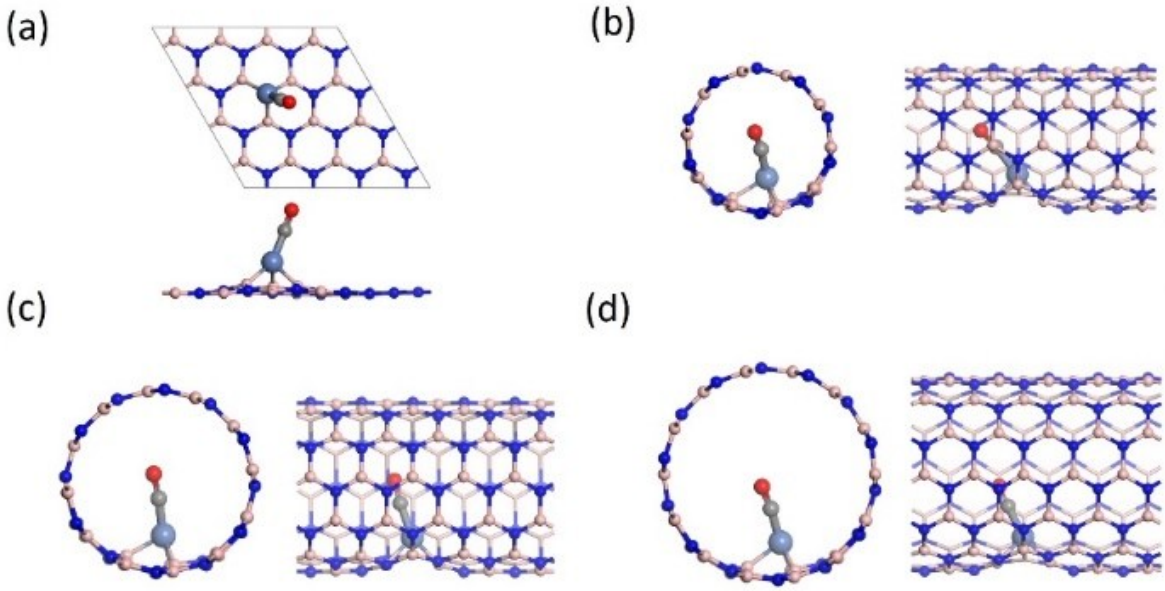

Figure S2. Similar to Figure S1 but for the CO adsorption on the catalyst sites.

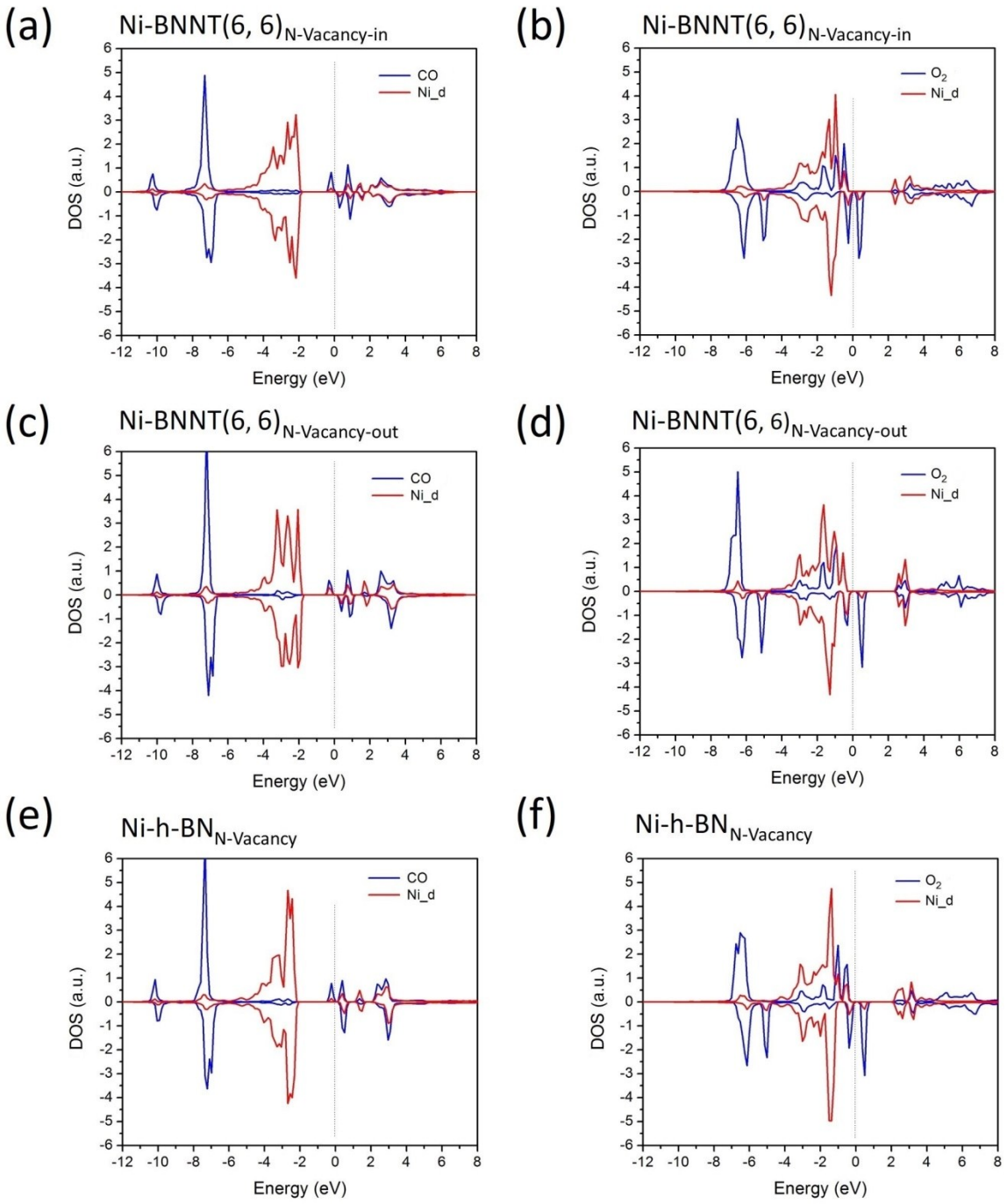

Figure S3. Spin-polarized density of states (DOS) of the most energetically favorable configurations of CO and O_2 adsorbed on the Ni-BNNT(6, 6)$_{N\text{-vacancy-in}}$, Ni-BNNT(6, 6)$_{N\text{-vacancy-out}}$, and Ni-h-BN$_{N\text{-vacancy}}$. Red and blue curves denote the *d*-projected DOS of the metal and the *p*-projected local DOS of CO/O_2, respectively.

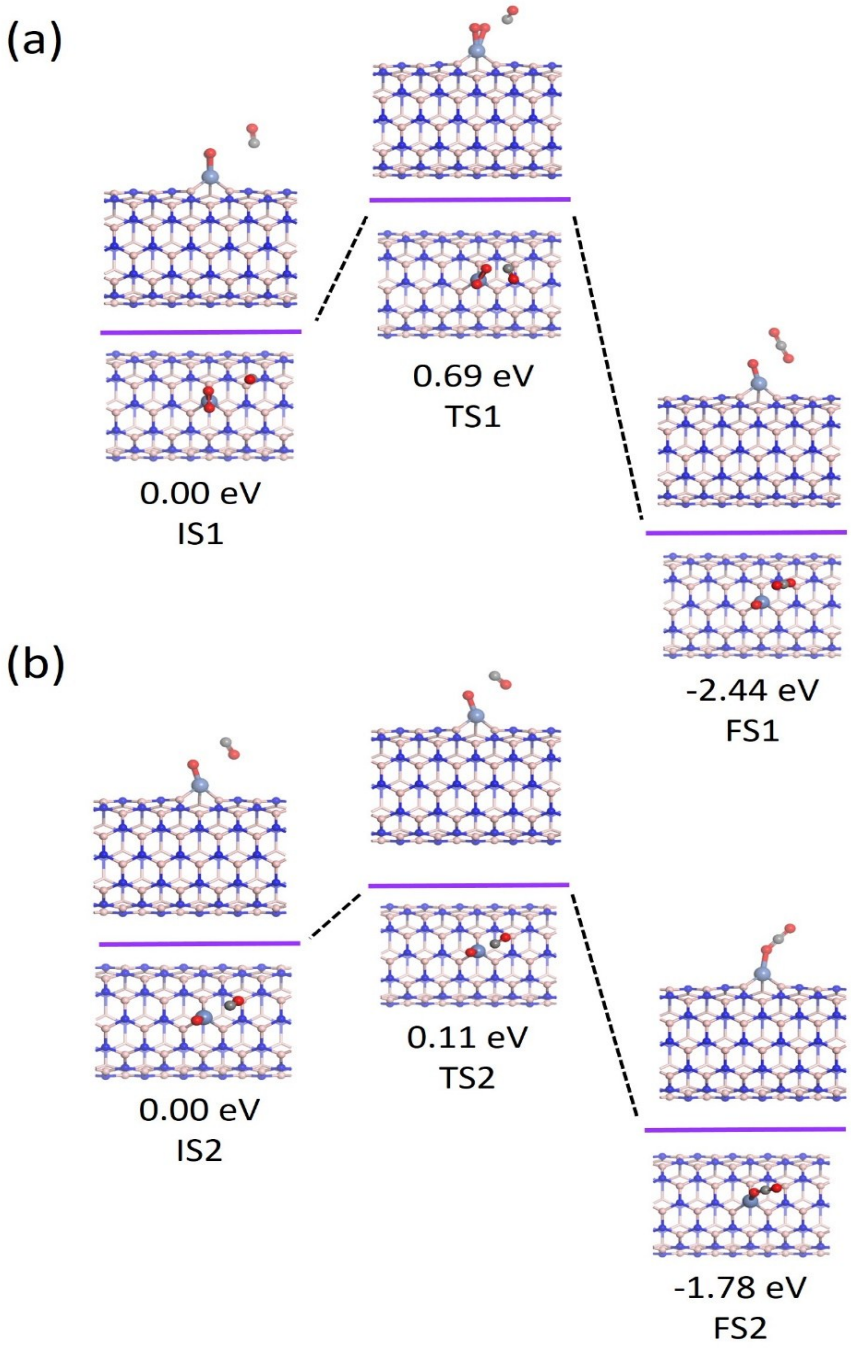

Figure S4. Geometries (side view) of initial state (IS), transition state (TS), and finial state (FS) along the minimum energy path (MEP) for the CO oxidation on Ni embedded on the exterior surface of BNNT (6, 6) with N-Vacancy via the ER mechanism. The energy changes between neighboring states are displayed.

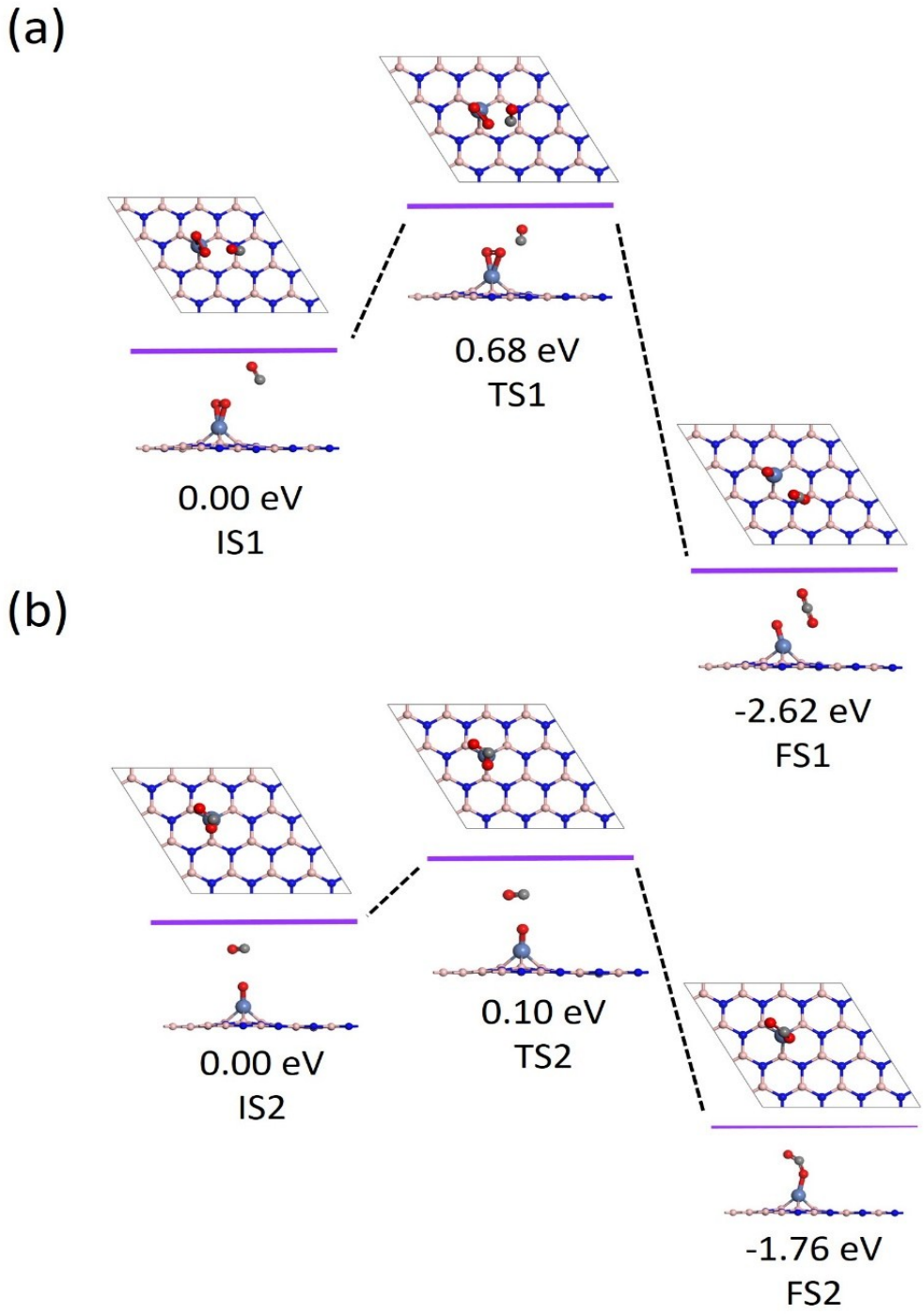

Figure S5. Geometries (side view) of initial state (IS), transition state (TS), and finial state (FS) along the MEP for the CO oxidation on Ni embedded h-BN with N-Vacancy via the ER mechanism. The energy changes between neighboring states are displayed.

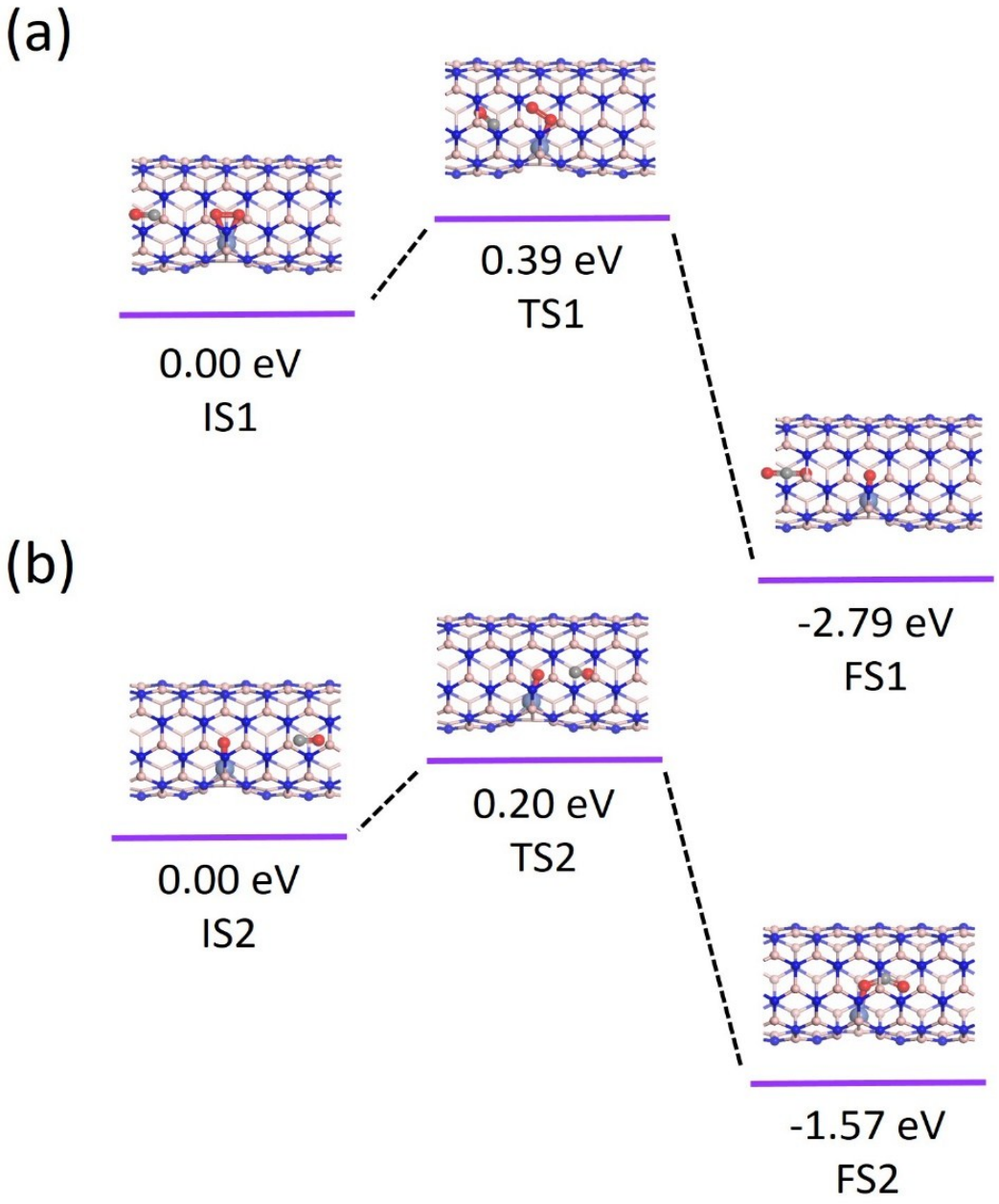

Figure S6. Geometries (side view) of initial state (IS), transition state (TS), and finial state (FS) along the MEP for the CO oxidation on Ni embedded in the interior wall of BNNT (5, 5) with N-Vacancy via the ER mechanism. The energy changes between neighboring states are displayed.

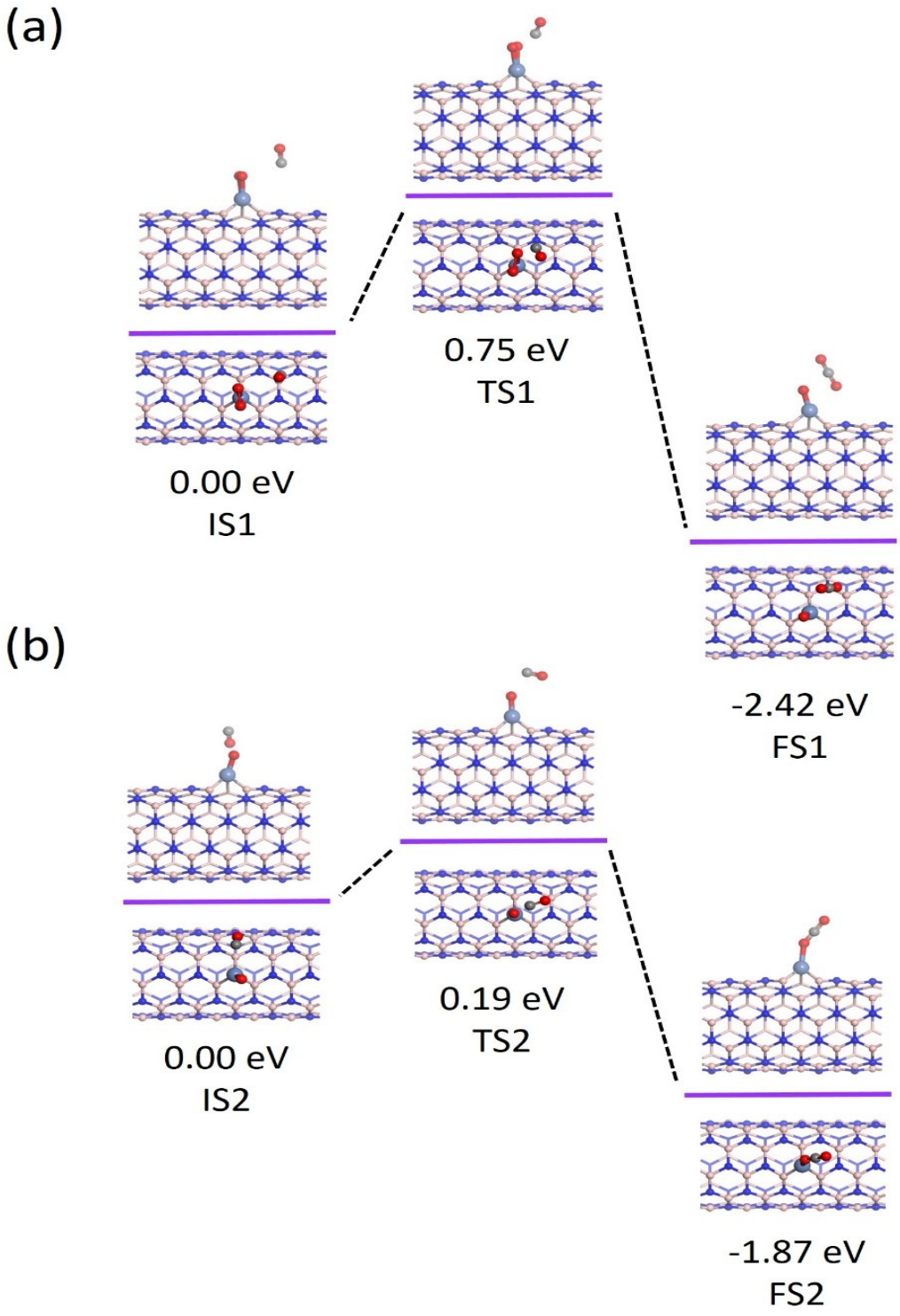

Figure S7. Geometries (side view) of initial state (IS), transition state (TS), and finial state (FS) along the MEP for the CO oxidation on Ni embedded on the exterior surface of BNNT (5, 5) with N-Vacancy via the ER mechanism. The energy changes between neighboring states are displayed.

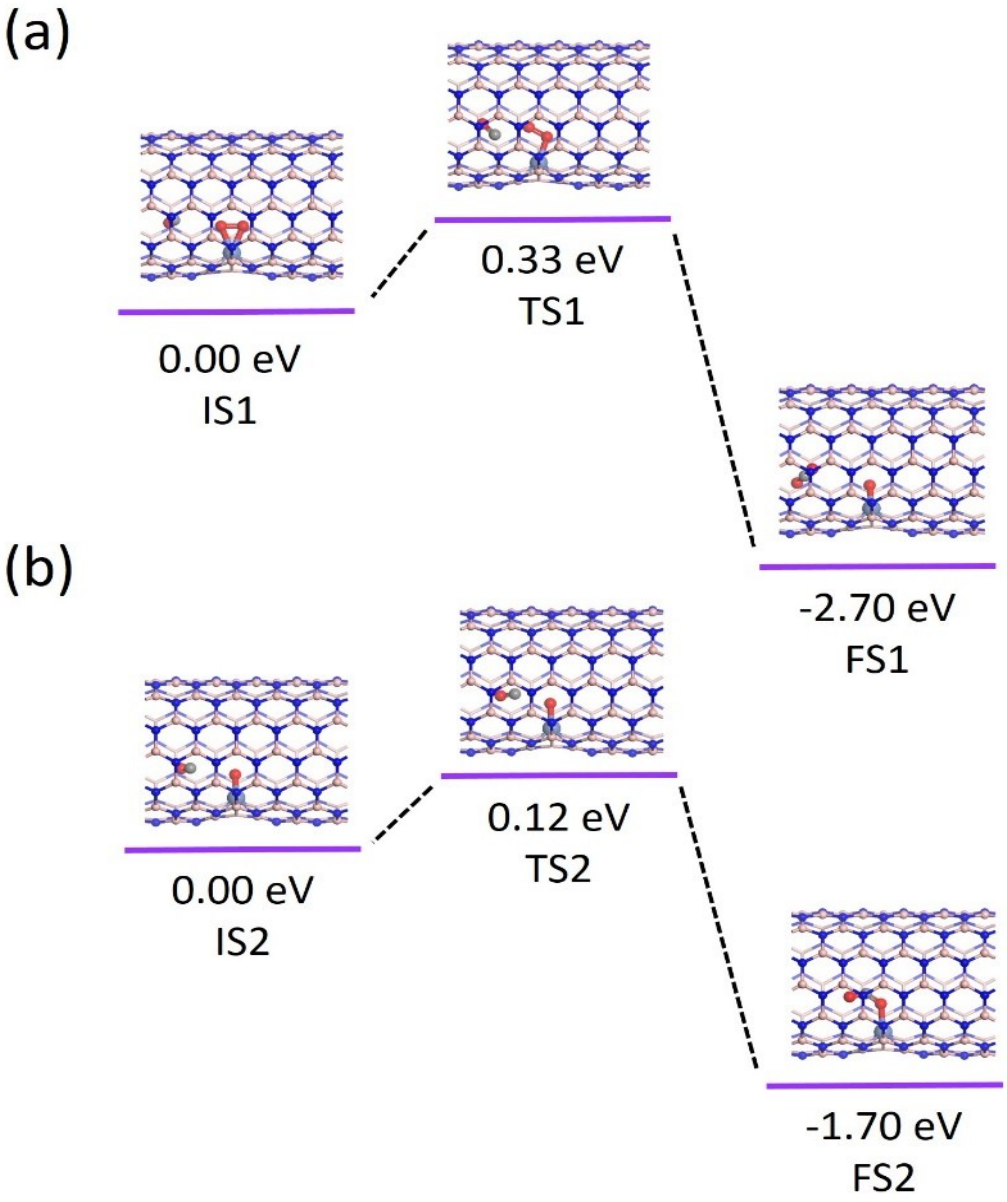

Figure S8. Geometries (side view) of initial state (IS), transition state (TS), and finial state (FS) along the MEP for the CO oxidation on Ni embedded in the interior wall of BNNT (7, 7) with N-Vacancy via the ER mechanism. The energy changes between neighboring states are displayed.

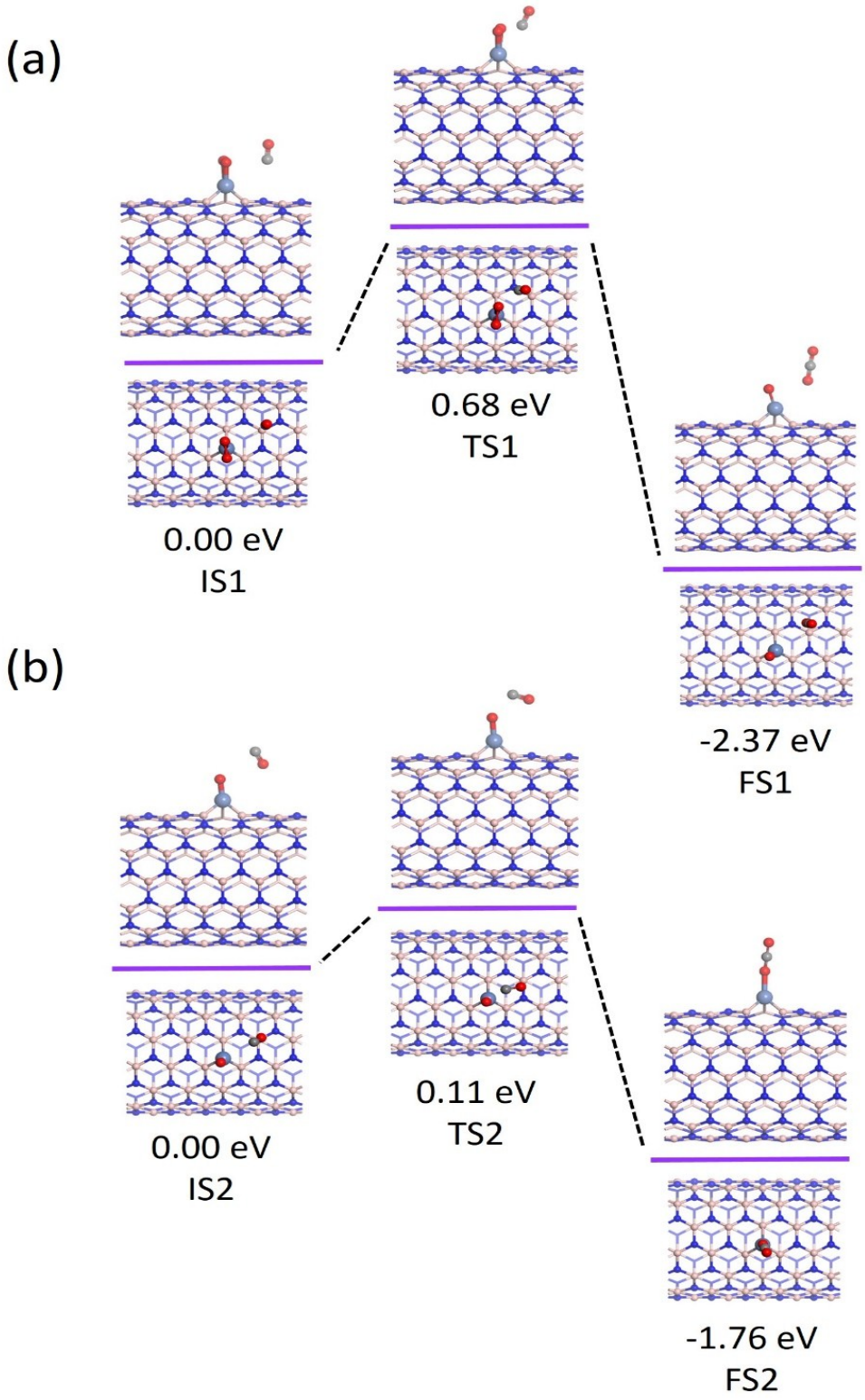

Figure S9. Geometries (side view) of initial state (IS), transition state (TS), and finial state (FS) along the MEP for the CO oxidation on Ni embedded on the exterior surface of BNNT (7, 7) with N-Vacancy via the ER mechanism. The energy changes between neighboring states are displayed.

Table S1 The binding energy (in eV) for O_2 and CO adsorbed on Ni-BNNT(5,5)$_{B\text{-}Vacancy\text{-}in/out}$ and Ni-BNNT(7,7)$_{B\text{-}Vacancy\text{-}in/out}$

substrates	E_b (CO)	E_b (O_2)
BNNT(5, 5)$_{B\text{-}Vacancy\text{-}in}$	*-1.05*	*-1.21*
BNNT(5, 5)$_{B\text{-}Vacancy\text{-}out}$	*-1.16*	*-0.81*
BNNT(7, 7)$_{B\text{-}Vacancy\text{-}in}$	*-0.88*	*-1.17*
BNNT(7, 7)$_{B\text{-}Vacancy\text{-}out}$	*-1.14*	*-1.16*

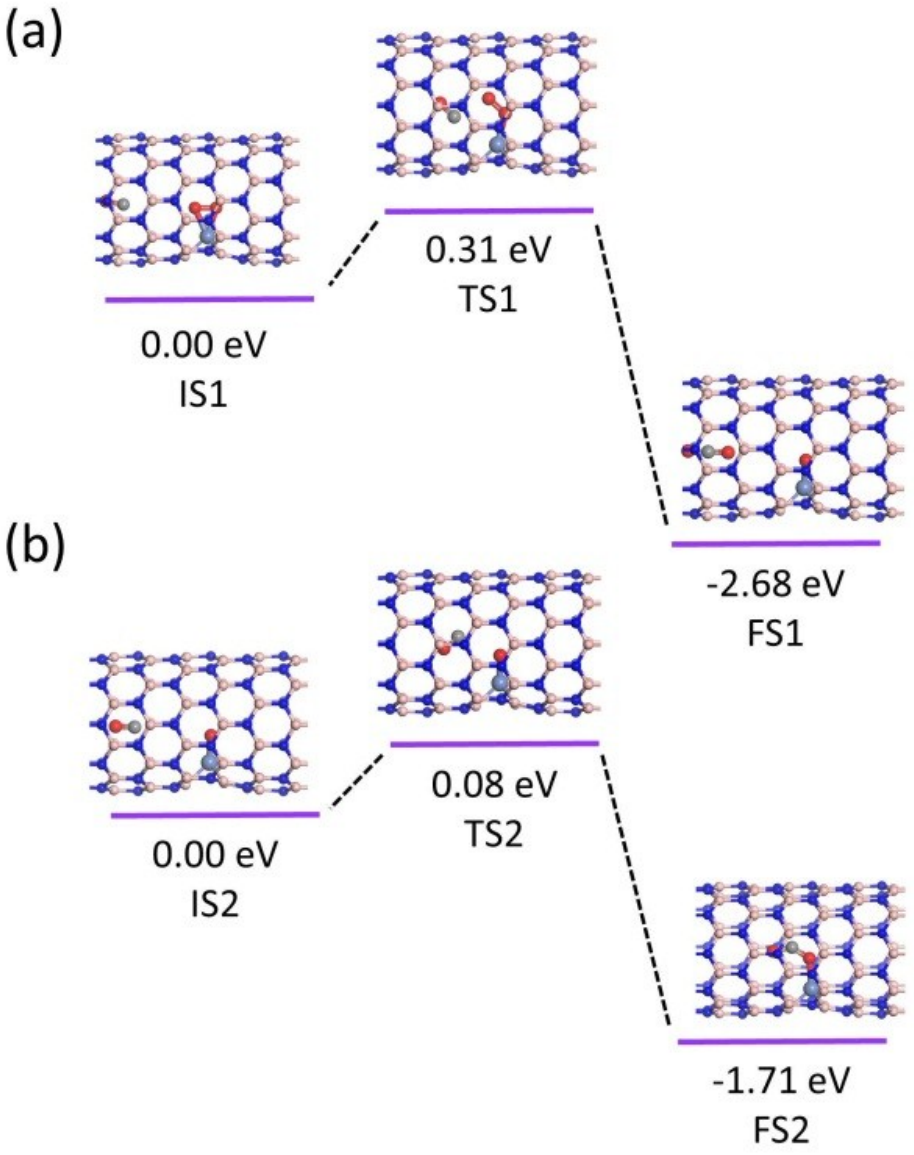

Figure S10 Geometries (side view) and energy profiles of initial state (IS), transition state (TS), and finial state (FS) along the minimum energy path for the CO oxidation on Ni embedded in the interior wall of BNNT (10, 0) with N-Vacancy via the ER mechanisms. The energy changes between neighboring states are displayed.

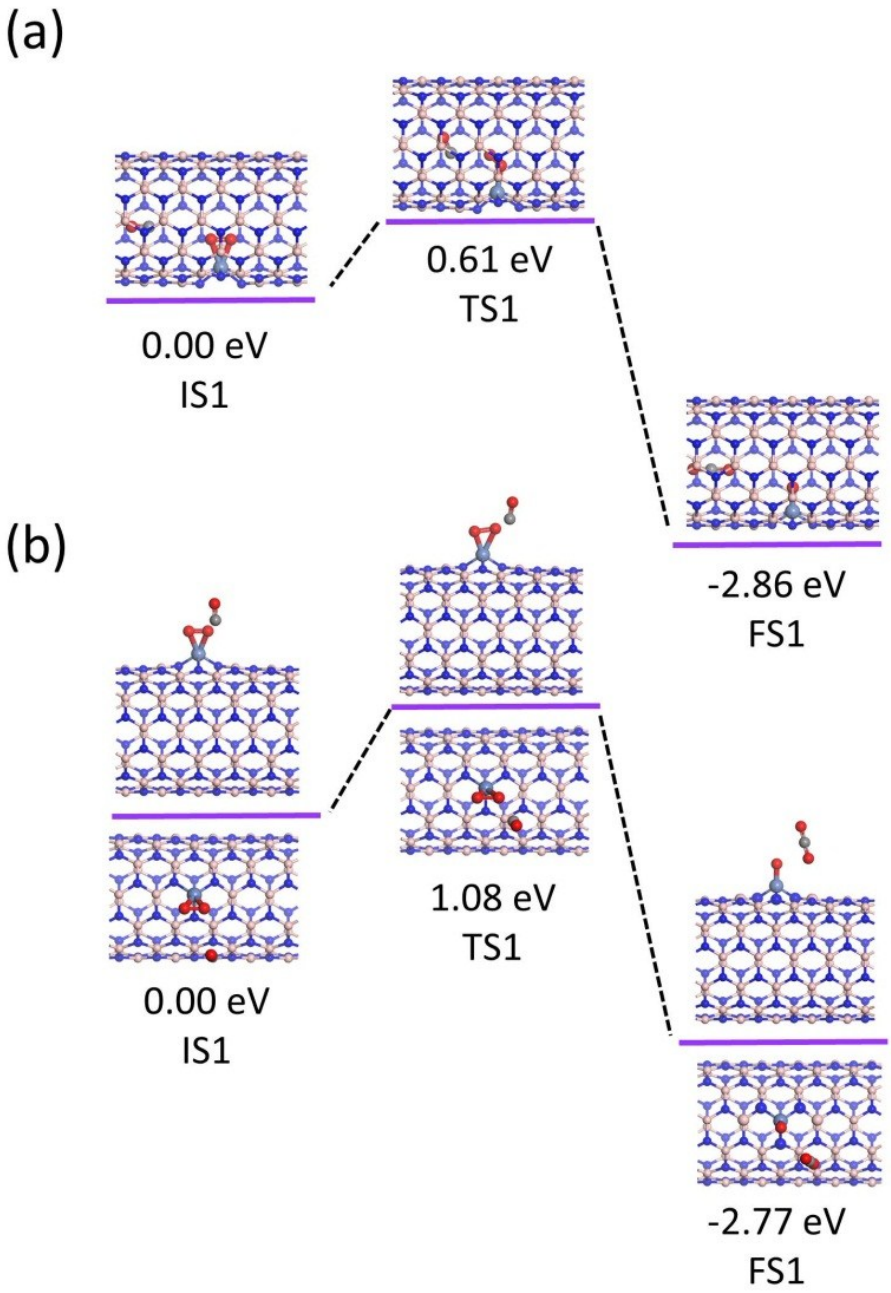

Figure S11 (a) Geometries (side view) and energy profiles of initial state (IS), transition state (TS), and finial state (FS) along the minimum energy path of the rate determining step for the CO oxidation on Ni embedded in the interior wall of BNNT (6, 6) with B-Vacancy via the ER mechanisms. (b) Geometries (side and top view) and energy profiles of initial state (IS), transition state (TS), and finial state (FS) along the minimum energy path of the rate determining step for the CO oxidation on Ni embedded in the exterior wall of BNNT (6, 6) with B-Vacancy via the ER mechanisms.

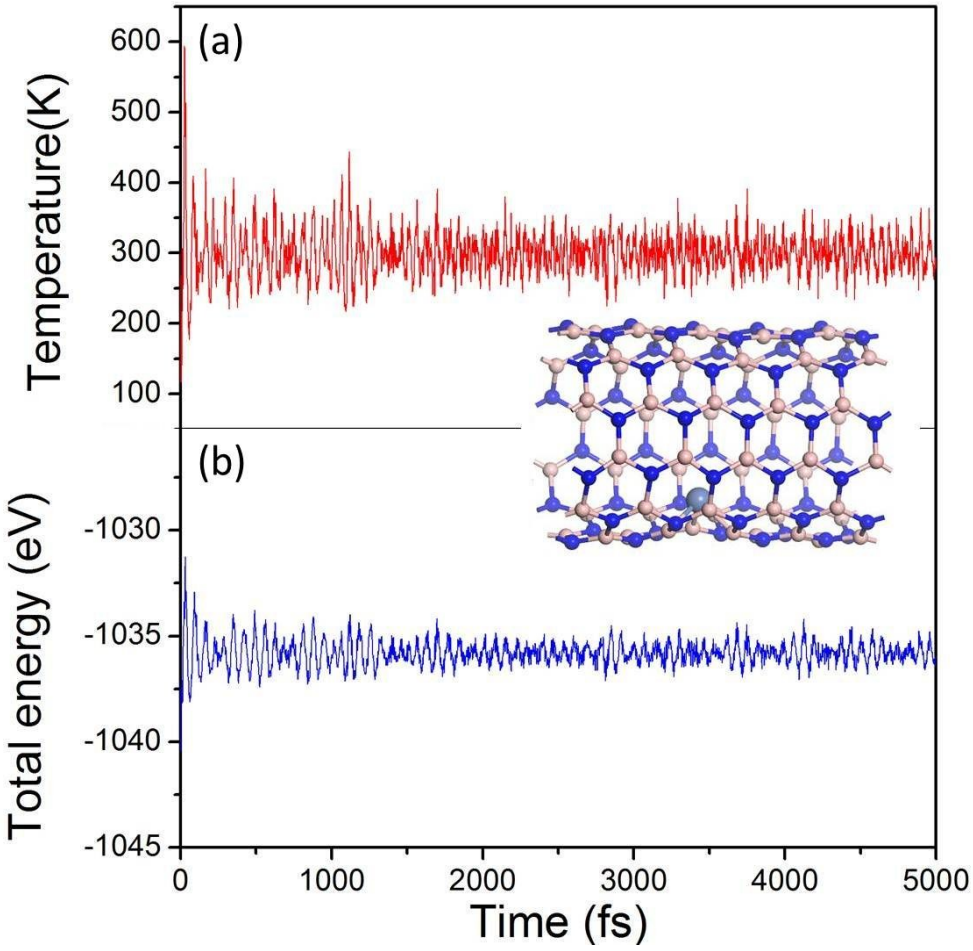

Figure S12 (a) Temperature and (b) total energy fluctuations vs. time in molecular dynamics simulations at 300 K for Ni embedded in the interior wall of BNNT (6, 6) with N-Vacancy. The inset refers to one of the typical structures of Ni-BNNT (6, 6)$_{\text{N-Vacancy-in}}$ during dynamics simulations.